Proc. Indian Acad. Sci. (*Chem. Sci.*), Vol. 113, Nos 5 & 6, October–December 2001, pp 621–631

Morpholinium intercalated vanadophosphates

SANJEEV SHARMA[a], A RAMANAN[a,*] and J J VITTAL[b]
[a]Department of Chemistry, Indian Institute of Technology,
New Delhi 110 016, India
[b]Department of Chemistry, National University of Singapore, Singapore
e-mail: aramanan@chemistry.iitd.ernet.in; aramanan57@hotmail.com

Abstract. The present paper reports the formation of two morpholinium (Morp) incorporated solids precipitated from aqueous vanadate solution acidifed with phosphoric acid: a zero-dimensional, mixed-valent phosphovanadate cluster containing solid, $[Morp]_6[P^VO_4 \subset V^{IV}{}_3V^V{}_{11}O_{32}(OH)_6].2H_2O$, **1** and a two-dimensional layered solid, $[Morp]_{0\cdot23}[V^{IV,V}OPO_4]1\cdot1H_2O$, **2**. While **2** precipitates out from the reaction mixture in the presence of a reducing agent hydrazine hydrate, **1** crystallises out in its absence.

Keywords. Intercalation; single crystal structure; vanadophosphate; morpholinium; vanadyl phosphate.

1. Introduction

Polyoxometalates form a rich class of inorganic materials exhibiting a range of molecular and electronic structural versatility, reactivity and relevance to catalysis, biology, medicine, geochemistry, material science and topology [1–4]. The metal oxide clusters invariably contain highly symmetrical core assemblies of MO_n units which often adopt quasi-spherical structures based on Archimedean and Platonic solids. Particularly interesting are the polyoxovanadates with hollow spheres which exhibit many different types of surface organization owing to a variety of metal macro-polyhedral fragments built of VO_4, VO_5, and VO_6 in addition to variable oxidation states V^{III}, V^{IV} and V^V. Polyoxovanadates frequently show interesting host–guest interaction [5]. Understanding the driving force for the formation of such clusters still remains a formidable challenge [6]. Many examples reported in the literature (see table 1) suggest that the role of organic counter-cations can become quite significant, especially if they can act as buffers, have the ability to reduce the vanadate and can provide suitable centres that can also participate in non-bonding interactions. Our group has been systematically investigating the formation of polyoxovanadates in the presence of several organic bases and salts that include morpholine, ethylenediamine, hexamethylenetetramine, triethanolammine tetramethyl ammonium bromide, tetraphenyl phosphonium bromide etc. In this paper we report our results on the formation of two novel phases in the system V–P–O incorporated with morpholinium (Morp) cation.

*For correspondence

Table 1. Selected polyoxovanadate clusters crystallized in the presence of organic cations

Polyoxovanadate cluster, $[VO_n]^{x-}$	Building blocks	Organic molecule	*p*H range	Ref.
Metavanadate chains, $[V^VO_3]$	V^VO_4	Morpholine or piperazine	8–10	7, 8
Cyclic metavanadate discrete $[V^V_4O_{12}]^{4-}$	V^VO_4	*t*-Butyl amine	10	9
Cyclic metavanadate chains $[V^V_4O_{11}]^{2-}$	V^VO_4	Tetraphenylphosphonium	5–6	10
Layered $[V^V_4O_{10}]^{2-}$	$V^VO_4 + V^{IV}O_5$	Ethylene diamine or diaminopropane	4–5	11, 12
Discrete $[V^{IV,V}_6O_{14}]^{2-}$	$V^{IV,V}O_6$	1,4-diazabicyclo[2,2,2]octan or tetramethyl ammonium	4–6	13
Discrete $[V^V_{12}O_{32}]^{4-}$	$V^VO_5 + V^VO_6$	Tetraphenyl-phosphonium and acetonitrile	4–6	14
Discrete decavanadate $[H_xV^V_{10}O_{28}]^{-(6-x)}$	$V^{IV,V}O_6$	Guanidine, pyridine, dodecyltri-methylamine, adenosinine or hexamethylenetetramine	4–6	8, 15–19
Discrete $[PV^V_{14}O_{42}]^{9-}$	$PO_4 + VO_5 + VO_6$	Guanidine or tetramethyl ammonium	4–5	20, 21
Discrete $[V^V_{18}O_{45}\,(V^{IV}O_4)]^-$	$V^VO_4 + V^VO_5$	*n*-Butyl ammonium	4–5	22
Layered $[V^{IV,V}_{18}O_{46}]^{5-}$	V^VO_5	Tetramethyl ammonium	5·0	23
Discrete $[HV_{22}O_{54}\,(ClO_4)]^{-6}$	$V^VO_5 + ClO_4$	Tetraethyl ammonium	Acidic	24

2. Experimental

The chemicals used were of reagent grade quality and were used without further purification. FTIR spectra were recorded on KBr pellets using Nicolet 5DX FTIR spectrophotometer. TG analyses were carried out using a Perkin–Elmer TGA7 system on well-ground samples in air or flowing nitrogen atmosphere with a heating rate of 10°C/min. Powder X-ray diffraction patterns were recorded on a Bruker AXS diffractometer using Kβ-filtered CuKα radiation. Scanning electron micrographs were recorded with the help of a Cambridge Stereoscan 360 microscope. In all the cases, the average oxidation state of vanadium as well as the total vanadium was determined by cerimetric titration.

2.1 *Synthesis of* $[Morp]_6[P^VO_4\,\grave{I}\,V^{IV}_3V^V_{11}O_{32}(OH)_6].2H_2O$, **1**

Compound **1** was synthesised from an aqueous solution containing V_2O_5 (2·75 mmol), phenylphosphonic acid (2·05 mmol) and morpholine (1·25 mmol) in 100 ml of water. The *p*H of the solution was adjusted to 4·0 by the addition of H_3PO_4 and refluxed at 80°C for 12 h. After keeping for five weeks, dark brown crystals appeared which were filtered off from the solution and washed with water followed by acetone, and dried in air. Yield: 30% based on vanadium. Polarizing microscope revealed the presence of uniform crystals with well-developed habits.

2.2 *Synthesis of* $[Morp]_{0·23}[V^{IV,V}OPO_4]1·1H_2O$, **2**

Compound **2** was synthesized from an aqueous solution containing V_2O_5 (2·75 mmol), phenylphosphonic acid (2·05 mmol) and morpholine (1·25 mmol) in 100 ml of water. Solid hydrazine hydrate (0·15 mmol) was added to the above solution. The *p*H of the solution was adjusted to 4·0 by the addition of H_3PO_4 and refluxed at 80°C for 12 h. After two weeks, flaky green-coloured crystals were precipitated out. The solid was filtered off from the solution and washed with water followed by acetone, and dried in air. Yield: 40% based on vanadium. Optical microscopic examination showed the presence of platy crystals with extensive agglomeration.

2.3 *X-ray crystallographic studies of* **1**

Single crystal diffraction studies were carried out on a Siemens SMART CCD diffractometer with a MoKα (0·71073 Å) sealed tube at 23°C for **1**. Crystals with dimensions of $0·35 \times 0·28 \times 0·25$ mm were used for diffraction experiments. A total of 16853 reflections in the theta range, 1·78–25·00 were used. The software SADABS was used for absorption correction and SHELXTL for space group and structure determination and refinements[25]. All the non-hydrogen atoms were refined anisotropically. Riding models were used to place the H atoms attached to carbon and nitrogen atoms. All the hydrogen atoms of the water molecules were located in the difference Fourier map and a common O–H distance and common isotropic thermal

Table 2. Crystal data and structure refinement for $\mathbf{PV_{14}}$.

Chemical formula	$C_{24}H_{68}N_6O_{50}PV_{14}$
Formula weight	1984·97
Crystal system	Monoclinic
Space group	*C*2/*c*
a(Å)	19·3541 (2)
b(Å)	14·1664 (2)
c(Å)	21·2290 (3)
α(°)	90·00
β(°)	92·03 (0)
γ(°)	90·00
V(Å^3)	5816·9 (1)
Temperature (K)	293(2)
Z	4
ρ_{calc} (g/cm^3)	2·267
ρ_{expt} (g/cm^3)	2.288
λ (Å)	0·71073
$R_1[I > 2\sigma(I)]$	0·0267
wR_2	0·0687
Theta range (°)	1·78 to 25·00
Total reflections	16853
F (000)	3964
Total parameters	445
GOF	1·159
Extinction coefficient	0·000040 (18)
Absorption coefficient (mm^{-1})	2·288

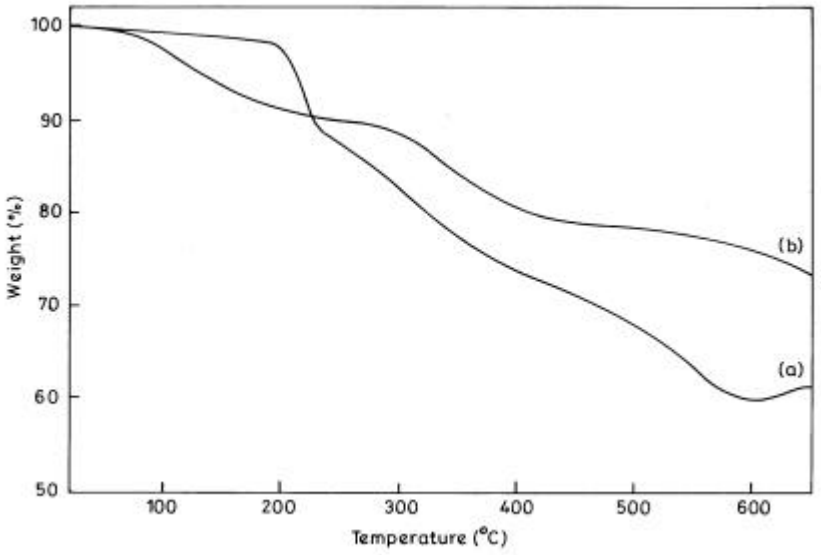

Figure 1. TG curves for (a) **1** and (b) **2**.

parameters of the oxygen atoms of the water molecules were refined. The hydrogen atoms attached to the $[PO_4 \subset V_{14}O_{38}]$ clusters could not be located. The least-squares refinement cycles on F^2 were performed until the model converged. The crystallographic data and the experimental details of **1** are listed in table 2.

3. Results and discussion

Chemical analysis showed that in both **1** and **2** vanadium was present in the mixed-valent state. Thermal analysis curves for **1** and **2** are shown in figure 1. For **1**, the loss of loosely packed lattice water occurs till 200°C and a broad weight loss corresponding to the decomposition of morpholine molecules occurs around 200–500°C. The composition of **1** derived from TG analysis agrees with the composition obtained from single crystal X-ray analysis. Inspection of the TGA plot for **2** reveals two dominant weight loss regions. The first loss (9·9%) occurs between 50 and 200°C due to water molecules. Following dehydration, the compounds decompose with loss of the organic portion at temperatures 200–500°C. Above this temperature vanadyl phosphate itself decomposes to unidentified products. On the basis of the TG analysis, the approximate composition for **2** is $[Morp]_{0\cdot23}[V^{VI,V}OPO_4]1\cdot1H_2O$. Both **1** and **2** showed characteristic vibrational features similar to polyoxovanadates and vanadyl phosphates respectively reported in the literature [7,8]. For **1**, symmetric and asymmetric stretching of the different kinds of V–O bonds are observed in the following regions: The terminal V–O bonds are in the range 990–975 cm^{-1}; the strong bands at 850–740 and 690 cm^{-1} are assigned to the anti-symmetric stretching vibrations of V–O–V features. The bands around 3460, 3300, 2930, 2700, 2510, 1610, 1590, 1450, 1300, 1092 and 1040 cm^{-1} indicate the presence of morpholinium cations and water molecules. V–O symmetric stretching and V–O–V anti-symmetric vibrational mode occur at 960(*m*), 925(*sh*), 900, 880, 800, 650(*sh*), 590(*m*),

500(*m*) and 450 cm^{-1}. For **2**, the peaks around 3420, 3280, 3000, 2850, 2730, 2520 1615, 1560, 1455, 1400, 1310, 1100 and 1040 cm^{-1} are associated with morpholinium cations. The strong band around 990 and 1055 cm^{-1} are assigned to ν_3 of PO_4 groups. The bands occurring around 990 cm^{-1} are due to V=O stretch. The broad, weak band around 680 cm^{-1} is due to V–O–P lattice. SEM micrographs (figure 2) of **1** indicate the formation of well-defined cubic block-like crystals, while for **2** the formation of platy crystals, a habit characteristic of layered vanadyl phosphate is observed.

3.1 *Description of the structure of **1***

Crystallographic data for **1** are given in table 2 and the atomic positional parameters of **1** are given in table 3. Single crystal X-ray diffraction of **1** reveals the presence of six morpholinium cations, $[C_4H_{10}NO]^+$, and a discrete molecular anion, $[PO_4 \subset V_{14}O_{38}]^{6-}$ that has a central cavity encapsulating an almost regular PO_4 tetrahedron. The three electron reduced oligomeric anion possesses a crystallographic 2-fold symmetry and the atoms P(1), V(2), V(7), O(2) and O(7) are present on the 2-fold axis. Figure 3 shows an ORTEP view of the anion in **1**. The vanadium oxo-anion cluster contains 12 VO_6 octahedra, two VO_5 square pyramids and one PO_4 tetrahedra where the two square pyramids and the tetrahedra occur along the two fold axis of the molecular symmetry like in the "bi-capped Keggin" anions reported in the literature. The central PO_4 tetrahedron shares its oxygen atoms with four V_3O_{13} units, each of which is made of three edge-sharing VO_6 octahedra. These four V_3O_{13} units are linked to each other by corner sharing. The two VO_5 square pyramids capped along the molecular axis share through edges to the neighbouring

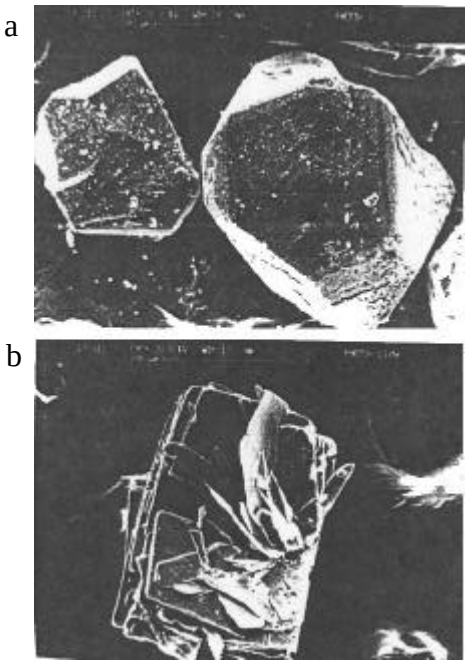

Figure 2. SEM photographs of (a) **1** and (b) **2**.

Table 3. Atomic coordinates ($\times 10^4$) and equivalent isotropic displacement parameters ($Å^2 \times 10^3$) of **1**.

Atom	*x*	*y*	*z*	U_{eq}
V(1)	0	−93(1)	2500	18(1)
V(2)	1296(1)	937(1)	2822(1)	19(1)
V(3)	447(1)	923(1)	1362(1)	17(1)
V(4)	1538(1)	2565(1)	1683(1)	18(1)
V(5)	871(1)	2603(1)	3952(1)	19(1)
V(6)	1280(1)	4273(1)	2856(1)	17(1)
V(7)	251(1)	4284(1)	1311(1)	18(1)
V(8)	0	5308(1)	2500	19(1)
P(1)	0	2598(1)	2500	14(1)
O(1)	0	−1225(2)	2500	28(1)
O(2)	1795(1)	81(1)	3057(1)	25(1)
O(3)	453(1)	94(1)	840(1)	26(1)
O(4)	2268(1)	2741(1)	1352(1)	26(1)
O(5)	1284(1)	2472(1)	4616(1)	27(1)
O(6)	1860(1)	5080(1)	2933(1)	26(1)
O(7)	545(1)	5111(1)	871(1)	26(1)
O(8)	0	6444(2)	2500	28(1)
O(9)	833(1)	225(1)	2093(1)	18(1)
O(10)	421(1)	472(1)	3186(1)	19(1)
O(11)	569(1)	1981(1)	2220(1)	18(1)
O(12)	1882(1)	1554(1)	2273(1)	23(1)
O(13)	1359(1)	1792(1)	3426(1)	21(1)
O(14)	1199(1)	1535(1)	1182(1)	21(1)
O(15)	−181(1)	1781(1)	996(1)	21(1)
O(16)	1658(1)	3398(1)	2411(1)	20(1)
O(17)	980(1)	3406(1)	1320(1)	21(1)
O(18)	1475(1)	3672(1)	3659(1)	21(1)
O(19)	336(1)	3218(1)	3023(1)	17(1)
O(20)	290(1)	3663(1)	4226(1)	21(1)
O(21)	742(1)	4745(1)	2136(1)	19(1)
O(22)	−477(1)	4984(1)	1735(1)	19(1)
O(23)	1120(1)	7818(1)	3954(1)	30(1)
C(1)	1099(2)	6814(2)	3970(1)	33(1)
C(2)	747(2)	6467(2)	4558(1)	36(1)
N(1)	37(1)	6864(2)	4572(1)	29(1)
C(3)	43(2)	7913(2)	4500(1)	32(1)
C(4)	429(2)	8177(2)	3915(1)	32(1)
O(24)	2959(1)	−133(2)	395(1)	33(1)
C(5)	2361(2)	427(2)	513(1)	29(1)
C(6)	2254(2)	1178(2)	17(1)	31(1)
N(2)	2193(1)	728(2)	−619(1)	28(1)
C(7)	2801(2)	114(2)	−735(1)	33(1)
C(8)	2881(2)	−601(2)	−209(1)	36(1)
O(25)	1436(1)	7114(2)	1245(1)	33(1)
C(9)	1885(2)	7881(2)	1114(1)	32(1)
C(10)	1783(2)	8681(2)	1564(1)	32(1)
N(3)	1910(1)	8355(2)	2227(1)	30(1)
C(11)	1498(2)	7490(2)	2363(1)	35(1)
C(12)	1614(2)	6755(2)	1862(1)	34(1)
O(1S)	1034(1)	−270(2)	−341(1)	45(1)

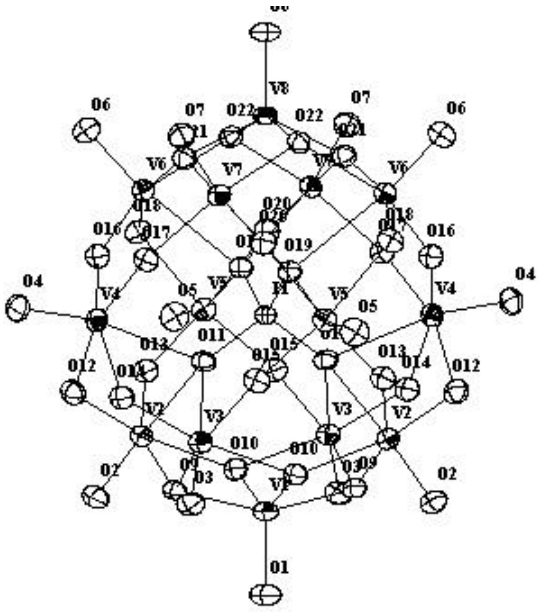

Figure 3. ORTEP view of the anionic cluster in **1**.

V_3O_{13}. The results of the X-ray structure analysis reveal that among each of these units, the V(2) of the VO_5 square pyramid show a shorter V–V metal distances in the range 2·950–2·965 Å with the four vanadium (V(3),V(3A), V(4) and V(4A)) of the VO_6; there is no short V–V interaction either between the four VO_6 octahedra occurring on the *xz*-plane or the four VO_6 octahedra among the two units. Selected bonding parameters of the anion are listed in table 4. The V=O, V–O(m_1), V–O(m_2) and V–O(m_3) bond distances are in the range of 1·60–1·62, 1·73–1·94, 1·83–2·05 and 2·35–2·39 Å respectively, indicating the expected trend of increasing V–O bond length for one- < two- < three- < four-coordinated oxygen as reported earlier[15–18]. The central PO_4 tetrahedral environment involves O–P–O angles ranging from 108·5–110·8° and P–O bond distances ~ 1·54 Å. Our attempts to refine the protons attached to cluster oxygens were not successful. In the mixed-valence anion, $[PO_4 \subset V^{IV}{}_3V^{V}{}_{11}O_{32}(OH)_6]^{6-}$ the three V^{IV} centres are statistically delocalized over the twelve octahedral and two square pyramidal sites.

An interesting feature of this structure is that each anion is surrounded by six morpholinium cations with its N atoms directed towards the O_t atoms of the anion by means of non-bonding interactions (see figure 4). The shortest non-bonding distance 1·857(6) Å is between O(20) of the anionic cluster and H(3C) of the morpholinium N–H hydrogen atom. The oxygen atoms O(3), O(4), O(5), O(9), O(16), O(18), O(20) and O(22) of the cluster anions are involved in close contacts of the type, X–H–O (X = N, C) and the distances range from 1·857 to 2·370 Å. The observed non-bonding strong and medium O–H interactions stemmed from N–H hydrogen atoms of the morpholinium cations and the weak interactions are due to C–H–O interactions. All the N–H hydrogen atoms of the morpholinium ions are participating in weak hydrogen bonding, mostly to the anionic cluster.

Table 4. Selected bond angles (°) and bond distances (Å).

Angles		Distances	
PO_4			
O(19)–P(1)–O(19)#1	110·59(13)	P(1)–O(11)	1·5424(17) × 2
O(19)–P(1)–O(11)#1	109·51(9)	P(1)–O(19)	1·5411(16) × 2
O(19)#1–P(1)–O(11)#1	108·18(9)		
O(11)#1–P(1)–O(11)	110·86(14)		
P(1)–O(11)–V(3)	127·09(9)		
P(1)–O(11)–V(4)	124·99(10)		
P(1)–O(11)–V(2)	124·16(9)		
P(1)–O(19)–V(5)	123·60(9)		
P(1)–O(19)–V(7)#1	126·19(9)		
P(1)–O(19)–V(6)	123·56(9)		
VO_5			
O(1)–V(1)–O(10)	115·95(6)	V(1)–O(1)	1·604(3)
O(1)–V(1)–O(10)#1	115·95(6)	V(1)–O(9)	1·9097(17) × 2
O(10)–V(1)–O(10)#1	128·11(11)	V(1)–O(10)	1·8278(17) × 2
O(1)–V(1)–O(9)#1	103·62(5)		
O(10)–V(1)–O(9)#1	84·06(7)		
O(10)#1–V(1)–O(9)#1	84·12(7)		
O(1)–V(1)–O(9)	103·62(5)		
O(10)–V(1)–O(9)	84·12(7)		
O(10)#1–V(1)–O(9)	84·06(7)		
O(9)#1–V(1)–O(9)	152·77(11)		
VO_6			
O(2)–V(2)–O(13)	105·37(9)	V(2)–O(2)	1·6193(18)
O(2)–V(2)–O(12)	99·96(9)	V(2)–O(9)	2·0296(17)
O(13)–V(2)–O(12)	95·99(9)	V(2)–O(10)	1·9965(17)
O(2)–V(2)–O(10)	97·98(9)	V(2)–O(11)	2·3810(17)
O(13)–V(2)–O(10)	89·05(8)	V(2)–O(12)	1·871(2)
O(12)–V(2)–O(10)	159·33(8)	V(2)–O(13)	1·7652(18)
O(2)–V(2)–O(9)	96·02(8)		
O(13)–V(2)–O(9)	155·91(8)		
O(12)–V(2)–O(9)	91·02(8)		
O(10)–V(2)–O(9)	76·93(7)		
O(2)–V(2)–O(11)	164·89(8)		
O(13)–V(2)–O(11)	89·35(7)		
O(12)–V(2)–O(11)	74·64(7)		
O(10)–V(2)–O(11)	85·42(7)		
O(9)–V(2)–O(11)	70·30(6)		
Morp			
C(1)–O(23)–C(4)	109·2(2)	O(23)–C(1)	1·423(4)
O(23)–C(1)–C(2)	110·9(2)	O(23)–C(4)	1·430(4)
N(1)–C(2)–C(1)	109·6(2)	C(1)–C(2)	1·524(4)
C(2)–N(1)–C(3)	111·3(2)	C(2)–N(1)	1·487(4)
N(1)–C(3)–C(4)	109·6(2)	N(1)–C(3)	1·494(4)
O(23)–C(4)–C(3)	110·6(2)		

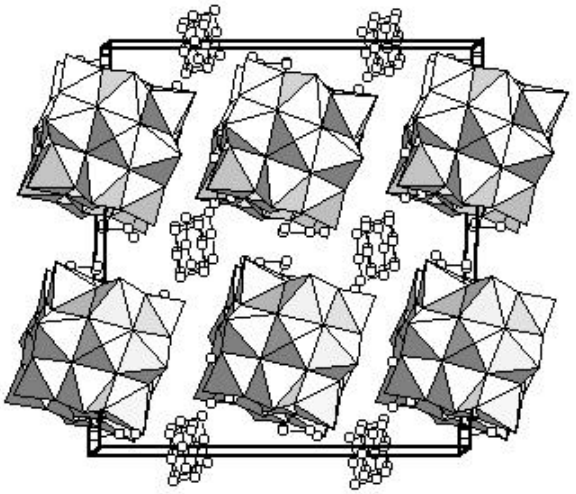

Figure 4. Unit cell packing diagram of **1**.

3.2 *Structure of morpholinium intercalated vanadyl phosphate, **2***

Compound **2** synthesised from aqueous solution under reducing condition yielded platy materials. Since suitable single crystals could not be obtained, structural analysis was carried out using powder X-ray diffraction data. X-ray diffractogram of **2** (figure 5) confirmed that it is a layered compound as signalled by the characteristic preferred orientation of low angle reflections and the multiple orders of the most intense peak. A 7·75 Å interlayer distance appears to be consistent with a structure in which morpholinium molecules are intercalated in between the vanadyl phosphate layers. FTIR spectra also confirm the presence of morpholinium cation in **2** (figure 6). Though solution studies indicate the occurrence of phosphovanadates in the ratios of V/P < 14, very few have been successfully crystallised [7,8]. Solutions with *p*H < 4 have invariably resulted in vanadyl phosphates. In the case of **2**, the amount of phosphoric acid in the solution was much higher than in the synthesis of **1**.

Isolation of the polyoxovanadates in the presence of organic bases/salts appears to be interesting. A number of metavanadates, decavanadates, and other isopolyvanadates in addition to several fully oxidized and mixed-valent high nuclear polyoxovanadate clusters have been crystallized from acidified, aqueous vanadate solution depending on the *p*H and oxidation state of vanadium (see table 1). The role of organic base in dictating the final structure of the solids either in determining the shape and size of the molecular cluster or occurring as a counter cation but influence the packing/linking of the inorganic anionic cores is important to understand the self-assembly process taking place in aqueous vanadate solution. We have been investigating the formation of polyoxovanadates by varying *p*H of the initial solution, the molar ratio of the starting materials, the oxidation state of vanadium, and organic bases with varying geometry – planar to spherical. Attempts were made to grow single crystals through solution evaporation or hydrothermal synthesis. Except for a few phases, we invariably obtained materials which were either amorphous precipitates or products that are difficult to characterize.

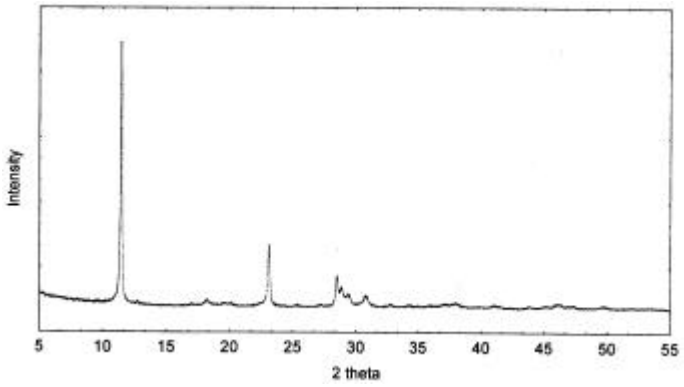

Figure 5. Powder X-ray diffraction pattern of **2**.

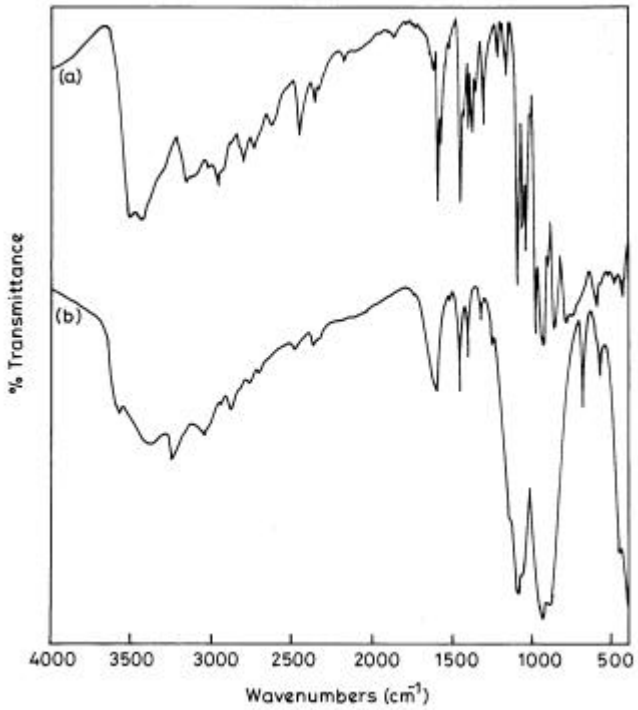

Figure 6. FTIR spectra of (a) **1** and (b) **2**.

Our earlier work[7] on V–O system showed that use of morpholine led to two products: metavanadate chains at *p*H ~ 8 and morpholinium incorporated mixed-valent cluster, $[V_{15}O_{42}]^{6-}$ at *p*H ~ 4. In this study we attempted to synthesize new phases in the V–P–O system. Our results have shown that under acidic conditions where V/P ratio is much higher $[PV_{14}O_{42}]^{6-}$ is the only stable cluster (as in compound **1**) which could be crystallised. At lower V/P ratio as in **2** (use of hydrazine hydrate has increased the pH to higher values and hence more H_3PO_4 was required to maintain the *p*H ~ 4·0) the most

stable phase appeared to be morpholinium intercalated layered vanadyl phosphate. Surprisingly, the same phase could not be synthesised by directly reacting morpholine with vanadyl sulphate or morpholine, V_2O_5 and H_3PO_4 by solvent evaporation or hydrothermal routes at lower *p*H with V/P ~ 1. **1** is the first example of a mixed-valent vanadophosphate cluster.

Acknowledgements

SS thanks the Department of Science and Technology (DST), New Delhi for a fellowship and AR acknowledges them for financial support.

References

1. Pope M T 1983 *Heteropoly and isopoly oxometalates* (Berlin: Springer)
2. Pope M T and Muller A 1991 *Angew. Chem., Int. Ed. Engl.* **30** 34
3. Klemperer W G, Marquart T A and Yaghi O M 1992 *Angew. Chem., Int. Ed. Engl.* **31** 49
4. Pope M T and Muller A (eds) 1994 In *Polyoxometalates: From platonic solids to anti-retroviral activity* (Dordrecht: Kluwer)
5. Muller A, Peters F, Pope M T and Gatteschi D 1998 *Chem. Rev.* **98** 239
6. Livage J 1998 *Coord. Chem. Rev.* **178** 999
7. Duraisamy T, Ohja N, Ramanan A and Vittal J J 1999 *Chem. Mater.* **11** 2339
8. Duraisamy T, Ramanan A and Vittal J J 2000 *Crystal Eng.* **3** 237
9. Roman P, Jose A S, Luque A and Gutierrez-Zorrillla A M 1993 *Inorg. Chem.* **32** 775
10. Sharma S, Ramanan A, Zavalij P and Whittingham M S (in preparation)
11. Zhang Y O, Connor C J, Haushalter R C and Clearfield A 1996 *Chem. Mater.* **8** 595
12. Zhang Y, Haushalter R C and Clearfield A 1996 *Inorg. Chem.* **35** 4950
13. Fazar L N, Koene B E and Taylor N J 1996 *Chem. Mater.* **8** 327
14. Day V W, Klemperer W G and Yaghi O M 1989 *J. Am. Chem. Soc.* **111** 4518
15. Tyroselova J, Kuchta L and Pavelcik F 1996 *Acta. Crystallogr.* **C52** 17
16. Wang X, Liu H X, Xu X X and You X Z 1993 *Polyhedron* **12** 77
17. Arrieta J M 1992 *Polyhedron* **11** 3045
18. Janauer G G, Dobey A D, Zavalij P Y and Whittigham M S 1997 *Chem. Mater.* **9** 647
19. Capperelli M V, Goodgame David M L, Hayman P B and Skapski A C 1986 *Chem. Commun.* 776
20. Kato R, Kobayashi A and Sasaki Y 1980 *J. Am. Chem. Soc.* **102** 6571
21. Khan M I, Zubieta J and Toscono P 1992 *Inorg. Chim. Acta* **193** 17
22. Suber L, Bonamico M and Fares V 1997 *Inorg. Chem.* **36** 2030
23. Koene B E, Taylor N J and Fazar L N 1999 *Angew. Chem., Int. Ed. Engl.* **38** 2888
24. Muller A, Diemann E, Krickmeyer E and Che S 1993 *Naturwissenschaften* **80** 77
25. Sheldrick G M 1996 SADABS, a software for empirical absorption correction, University of Gottingen, Gottingen, Germany; SHELXTL Reference Manual version 5.03, Siemens Energy and Automation, Inc., Analytical Instrumentation, Madison, WI